

THE SEMI-LEPTONIC DECAYS OF THE D MESON\*

W. Bacino, T. Ferguson,<sup>a)</sup> L. Nodulman,<sup>b)</sup> W. Slater and H. Ticho

Physics Department  
University of California, Los Angeles, California 90024

A. Diamant-Berger,<sup>c)</sup> G. Donaldson, M. Duro, A. Hall,<sup>d)</sup> G. Irwin,  
J. Kirkby, F. Merritt and S. Wojcicki

Stanford Linear Accelerator Center and Physics Department  
Stanford University, Stanford, California 94305

R. Burns,<sup>e)</sup> P. Condon<sup>f)</sup> and P. Cowell<sup>g)</sup>

Physics Department  
University of California, Irvine, California 92664

J. Kirz

Physics Department  
State University of New York, Stony Brook, NY 11794

Abstract

The electron energy spectrum in the process  $e^+e^- \rightarrow \psi''(3770) \rightarrow e^{\pm} + 2$  charged particles has been used to determine the D ( $56\%D^0 + 44\%D^+$ ) semi-leptonic branching ratio. Assuming the GIM model, we find the inclusive branching ratio  $b(D \rightarrow Xev) = 0.080 \pm 0.015$  and the state X to be dominated by K and  $K\pi$ . The fraction of  $K\pi ev$  is  $(37 \pm 16)\%$  if the  $K\pi$  system is entirely  $K^*(890)$ , or  $(55 \pm 21)\%$  if the  $K\pi$  system is non-resonant. Within the assumptions of the analysis, we calculate the D lifetime to be  $(2.5 \pm 1.6)10^{-13}$  sec.

---

\*Work supported in part by the National Science Foundation and by the Department of Energy under contract number DE-AC03076F00515

a) Current address: Cornell University, Ithaca, New York 14853

b) Current address: Argonne National Laboratory, Argonne, IL 60439

c) Permanent address: DPhPE, Saclay, France

d) Current address: Varian Associates, Palo Alto, California 94303

e) Current address: Hughes Aircraft Co., Newport Beach, California 92663

f) Current address: Lawrence Berkeley Laboratory, Berkeley, California 94720

g) Current address: Systems Control, Inc., Palo Alto, California 94303

We have studied the final states in the semi-leptonic decays of D mesons by means of the electron energy spectrum observed in  $e^+e^-$  annihilations.<sup>1)</sup> The analysis assumes the decays are predominantly  $D \rightarrow K(n\pi)ev$ ,  $n \geq 0$ , following the Glashow-Iliopoulos-Maiani<sup>2)</sup> (GIM) model. The value of the inclusive semi-leptonic branching ratio measures the strength of the non-leptonic enhancement analogous to that observed in K decays. Furthermore, since the rate  $\Gamma(D \rightarrow Kev)$  can be reliably calculated, the lifetimes of the  $D^0$  and  $D^+$  can be determined from their  $Kev$  branching ratios. Additional interest in these decay modes arises from the Quantum Chromodynamics (QCD) calculation of the mass and lifetime of the charmed quark, which uses the measured lepton momentum spectrum and  $b(D \rightarrow Xev)$ .<sup>4)</sup>

The data, recorded by the DELCO detector<sup>5)</sup> at SPEAR, is taken from the  $\psi''(3770)$  region,  $3.76 < E_{cm} < 3.78$  GeV. This facilitates our analysis for several reasons: the charm cross section is resonant and therefore can be well measured; the charmed particles are produced simply in  $D\bar{D}$  pairs (the  $D^0\bar{D}^0 : D^+D^-$  ratio is 0.56 : 0.44 according to phase space) with a known, small velocity ( $|P_D| \sim 0.26$  GeV/c). Therefore, the measurements suffer neither from uncertainties in the  $c \rightarrow D$  fragmentation nor from substantial Lorentz smearing.

For the purpose of this analysis, we select events with  $\geq 3$  observed charged particles of which one and only one is identified as an electron by having in-time Cerenkov and shower counter pulses. The minimum pulse-heights correspond to 0.7 photo-electrons for the Cerenkov counter and 0.3 minimum-ionizing-particles for the shower counter. The candidate electron track is required to have at least one hit in the two innermost cylindrical

proportional chambers in order to decrease photon conversion backgrounds. To achieve unambiguous electron identification, we retain those events where only one track enters the triggered Cerenkov cell. A further requirement of at least one hit in the outer spark chambers (azimuthal view) ensures a momentum measurement accuracy of  $\sigma_p/P = \sqrt{(0.052)^2 + (0.080/P)^2}$ , where P (GeV/c) is the track momentum.

The electron momentum spectrum of the 596 events which satisfy these criteria is shown in Fig. 1. These data are not yet corrected for backgrounds or Cerenkov detection efficiency (Fig. 2). The predominant background source of high-energy electrons is electronic  $\tau$  decays<sup>6)</sup> (indicated by the solid line in Fig. 1). The remaining backgrounds come from two sources: hadronic events and two-photon processes. Our studies indicate the former consists largely of accidental coincidences of a hadronic track and a Cerenkov pulse, either from phototube dark current or  $\gamma$  conversions in the Cerenkov entrance (64% of the hadronic background). Other sources include  $\gamma$  conversions in the beam-pipe (15%), electrons from unidentified Dalitz pairs (12%),  $\delta$  ray production in the Cerenkov counter (4%), K decays (2%) and Compton scattering (2%). These spectra have been calculated separately and the combined shape and magnitude are compared with the electron spectrum observed in multi-prong events at the  $\psi(3100)$  (Fig. 3a). The discrepancy between the observed and predicted low-energy electron spectra introduces a small systematic uncertainty which has been included in our final quoted errors. The overall probability for a track to be improperly identified as a candidate electron is about  $2 \times 10^{-3}$ . At energies other than the  $\psi(3100)$  and  $\psi'(3685)$ , several QED processes lead to additional electron backgrounds. Calculations of the two-photon final

states,<sup>7)</sup>  $e^+e^-X$  ( $X = \mu^+\mu^-, \pi^+\pi^-, \eta, \eta'$ ), and  $\rho$  photoproduction,<sup>8)</sup>  $e^+e^- \rightarrow e^+e^-\rho$ , indicate a contribution of magnitude 0.14 relative to the background from hadronic events. The predicted background in the range  $3.50 < E_{\text{cm}} < 3.52$  (Fig. 3b) includes these QED calculations. The level of agreement of the background predictions with the data below charm threshold is a measure of the quality of similar calculations applied to the data of Fig. 1 (indicated by the dashed curve).

After subtracting the backgrounds and correcting for the Cerenkov detection efficiency, we obtain the electron energy spectrum from D decays (Fig. 4). This spectrum can be compared with several hypotheses for D semileptonic decays.<sup>9)</sup> As seen from Fig. 4a), the spectrum is incompatible with a single decay mode, whether it be  $D \rightarrow \pi e \nu$ ,  $D \rightarrow K e \nu$ <sup>10)</sup> or  $D \rightarrow K^*(890) e \nu$ . However, the observed spectrum agrees well with a mixture of these decay modes (Fig. 4b). In this fit we include a contribution from  $\pi e \nu$  (with a fixed fraction of  $2.0 \tan^2 \theta_c = 0.11$ <sup>11)</sup> relative to  $K e \nu$ ), since it is the only Cabibbo-suppressed mode whose electron spectrum could bias our results. After accounting for detection efficiencies and systematic errors, we measure<sup>12)</sup> the contributions  $(37 \pm 16)\%$ <sup>13)</sup> and  $(55 \pm 14)\%$  from  $K^*(890) e \nu$  and  $K e \nu$ , respectively. This result is insensitive to the  $\pi e \nu$  fraction but depends on the assumption of resonant  $K\pi$  production. A fit finds contributions of  $(55 \pm 21)\%$  and  $(38 \pm 19)\%$  from non-resonant  $K e \nu$  and  $K e \nu$ , respectively,<sup>14)</sup> with a  $\chi^2/\text{dof}$  of 8.4/15. The systematic uncertainties arising from the background subtraction are determined by varying the individual contributions while retaining compatibility with the data of Fig. 3 and with the experimental values of the  $\tau$  parameters.

The inclusive electronic branching ratio is determined from the

background-subtracted events using a Monte Carlo technique to calculate the detection efficiency. This efficiency is insensitive to the relative rates of the  $\pi$ , K and  $K\pi$  semi-leptonic modes for equal  $D^+$  and  $D^0$  contributions. After accounting for systematic errors, we obtain<sup>15)</sup>  $b(D \rightarrow X\text{ev}) = 0.080 \pm 0.015$ .

We have investigated the possible contribution of  $D \rightarrow K\pi\text{ev}$  by fitting the electron energy spectrum with this channel and varying fractions of  $K\text{ev}$ ,  $K^*\text{ev}$  and  $K\pi\text{ev}$ . In all fits the  $K\pi\text{ev}$  contribution is small (the largest value is  $(11^{+20}_{-11})\%$  of the total). This fraction corresponds to non-resonant  $K\pi\pi$  production; it decreases in the case of resonant production such as  $Q(1280)$  and  $K^{**}(1420)$ . In view of this small value it is unlikely that the decays  $D \rightarrow K(n\pi)\text{ev}$ ,  $n \geq 2$  constitute a significant fraction of the D semileptonic decays.

The measured value for  $b(D \rightarrow X\text{ev})$ , when compared with the naive free quark estimate of 0.20, suggests that the hadronic decay enhancement is weaker in charm-changing decays than in strange-particle decays. However, we stress that our measurement gives the average semi-leptonic branching ratios for an approximately equal sample of  $D^+D^-$  and  $D^0\overline{D^0}$  events and thus does not address itself to the question of equality of the  $D^+$  and  $D^0$  hadronic decay rates.<sup>16)</sup> The observation that the D semileptonic decays are dominated by the channels  $K\text{ev}$  and  $K\pi\text{ev}$  is in reasonable accord with theoretical expectations<sup>3)</sup> based on the GIM model. The calculations for  $\Gamma(D \rightarrow K\text{ev})$  predict  $1.4 \cdot 10^{11} \text{ sec}^{-1}$ , assuming  $F^*$  dominance of the form factor, or  $1.1 \cdot 10^{11} \text{ sec}^{-1}$  in the case of a constant form factor. Using the former value, we compute the D lifetime to be  $(2.5 \pm 1.6)10^{-13} \text{ sec.}$ , assuming equality of the  $D^+$  and  $D^0$  total decay rates. This value agrees with

recent QCD calculations which assume the lifetime of charmed hadrons is simply the charmed quark lifetime. This type of calculation is sensitive to the mass of the charmed quark. The authors of reference 4) found this mass to lie in range  $1.6 < m_c < 1.8 \text{ GeV}/c^2$ , using a preliminary version of these electron data.

#### Acknowledgements

We acknowledge the invaluable services of the Experimental Facilities Division, SPEAR Operations Group, and Stanford Linear Accelerator Computing Center. This work was supported in part by the U.S. National Science Foundation and the Department of Energy.

## References

- 1) See R. Brandelik et al., Phys. Lett. 70B 387 (1977) and J.M. Feller et al., Phys. Rev. Lett. 40, 274 (1978) for the results on this subject from DASP and the Pb Glass Wall experiment, respectively.
- 2) S.L. Glashow, J. Iliopoulos, and L. Maiani, Phys. Rev. D2, 1283 (1970).
- 3) M.K. Gaillard, B.W. Lee and J.L. Rosner, Rev. Mod. Ph. 47, 277 (1975), J. Ellis, J.K. Gaillard and D.V. Nanopoulos, Nucl. Phys. B100, 313 (1975), A. Ali and T.C. Yang, Phys. Lett. 65B, 275 (1976), I. Hinchliffe and C.H. Llewellyn-Smith, Nucl. Phys. B114, 45 (1976), V. Barger, T. Gottschalk and R. Phillips, Phys. Rev. D16, 746 (1977), W. Wilson, Phys. Rev. D16, 742 (1977), F. Bletzacker, M.T. Nieh and A. Soni, Phys. Rev. D16, 732 (1977), D. Fabirov and B. Stech, Nucl. Phys. B133, 315 (1978), G.L. Kane, K. Stowe and W.B. Rolnick, UM HE 77-25 (1978) (unpublished).
- 4) M. Suzuki, Nucl. Phys. B145, 420 (1978), N. Cabibbo and L. Maiani, Phys. Lett. 79B, 109 (1978), A. Ali and E. Pietarinen, DESY 79/12 (1979)(unpublished), N. Cabibbo, G. Corbo and L. Maiani, Rome University preprint 79-0279 (1979)(unpublished).
- 5) W. Bacino et al., Phys. Rev. Lett. 70B, 387 (1977).
- 6) We use the branching ratios,  $b(\tau \rightarrow e \nu_e \nu_\tau) = 0.16$  and  $b(\tau \rightarrow \geq 3\text{-charged-particles } \nu_\tau) = 0.26$ . In the subsequent error analysis these numbers are given systematic errors of  $\pm 0.03$  and  $\pm 0.06$ , respectively.
- 7) J. Vermaseren, Purdue University (private communication).
- 8) Rohini Godbole and J. Smith, CERN TH. 2648 (1979)(unpublished).
- 9) We have derived the theoretical spectra from the papers in ref. 2) of W. Wilson, A. Ali and T.C. Yang (setting the parameter  $\delta = 0$ ). The

Kev spectrum includes a form-factor dominated by  $F^{**}$  (although the shape is insensitive to this assumption) and the  $K^{**}$  ev spectrum assumes a V-A current.

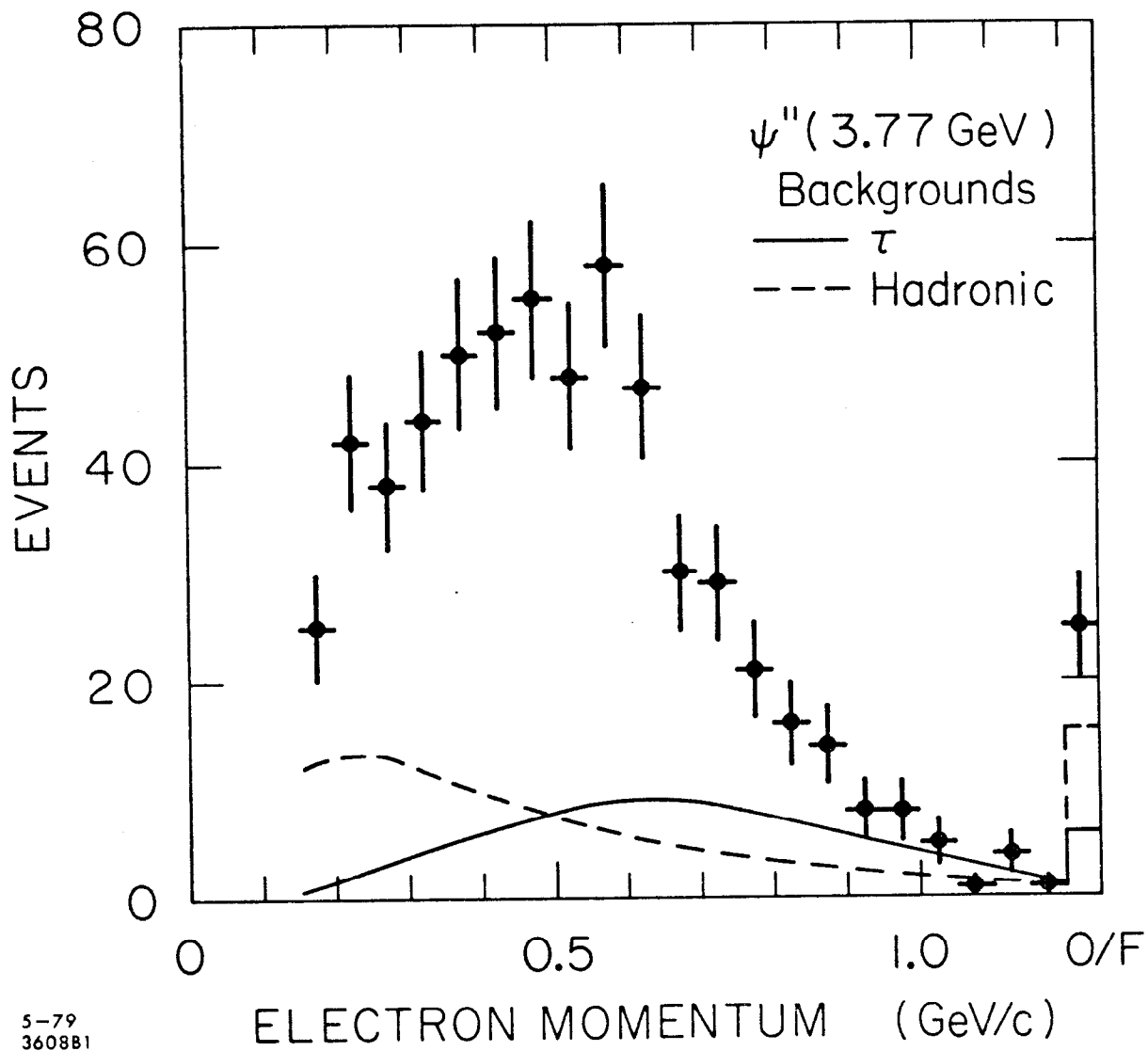
- 10) Although the Kev fit is acceptable by a  $\chi^2$  test, it displays a systematic shift toward high momenta. These point-to-point correlations are measured by an independent statistical parameter known as the 'run test', described in W.T. Eadie et al., Statistical Methods in Experimental Physics (North Holland, Amsterdam and London, 1971). When applied to the Kev fit of Fig. 4a), it associates a probability of  $5 \times 10^{-3}$  with the hypothesis of pure  $D \rightarrow K^{**}$ .
- 11) F. Bletacker, M.T. Nieh and A. Soni, Phys. Rev. D16, 732 (1977).
- 12) This measurement is strongly dependent on the V-A assumption. A V+A current hardens the electron spectrum and gives an acceptable fit with the single decay  $D \rightarrow K^{**}(890)$ ev.
- 13) The calculation of the  $K\pi$  fraction involves a small subtraction of the  $\pi\pi$  contribution.
- 14) A fit of the single decay mode  $D \rightarrow K\pi$ ev has a  $\chi^2/\text{dof} = 19.8/16$  and a 'run test' probability of  $2 \times 10^{-2}$ .
- 15) This measurement of  $b(D \rightarrow X\text{ev})$  follows the original Breit-Wigner analysis described in reference 5). The new value, which differs from our previous measurement of  $0.11 \pm 0.02$ , results from a larger electron background estimation. In particular, the  $\tau$  contribution was not included previously, since it was not known that the  $\psi''$  mass exceeded  $\tau^+\tau^-$  threshold.
- 16) M. Katuya and Y. Koide, Shizuoka Womens University preprint SH-78-05 (unpublished).



- 17) For a recent discussion of other experimental data bearing on the D lifetime, see S.G. Wojcicki, Proceedings of the SLAC Summer Institute on Particle Physics, SLAC Rep. 215, ed. by M. Zipf (1978).

Figure Captions:

1. The electron momentum spectrum from multi-prong events observed in the center-of-mass energy range,  $3.76 < E_{\text{cm}} < 3.78$  GeV. The solid curve indicates the predicted contribution from  $\tau$  decays (19% of the observed events). The dashed curve shows all other sources of background (24%).
2. The Cerenkov counter detection efficiency vs. electron momentum. The curve is drawn through the data points obtained from the final states  $e^+e^-$ ,  $e^+e^-\gamma$  and  $e^+e^-e^+e^-$ . The efficiency includes geometrical losses due to mirror edges.
3. a) The electron momentum spectrum from multi-prong events observed at the  $\psi$  (3100).  
b) The electron momentum spectrum observed in the energy range  $3.50 < E_{\text{cm}} < 3.52$  GeV. In both figures the dashed curve shows the predicted spectrum.
4. The electron momentum spectrum from D decays at the  $\psi''$ (3770). The curves have been fitted to the data below 1 GeV/c and correspond to the following hypotheses:
  - a)  $D \rightarrow \pi e \nu$  (dot-dashed curve,  $\chi^2/\text{dof} = 80.9/16$ ),  $D \rightarrow K e \nu$  (solid curve,  $\chi^2/\text{dof} = 23.4/16$ ),  $D \rightarrow K^{*}(890) e \nu$  (dashed curve,  $\chi^2/\text{dof} = 53.8/16$ ).
  - b) Contributions from  $D \rightarrow K e \nu$  (55%),  $D \rightarrow K^{*}(890) e \nu$  (39%) and  $D \rightarrow \pi e \nu$  (6%) ( $\chi^2/\text{dof} = 11.2/15$ ).



5-79  
3608B1

Fig. 1

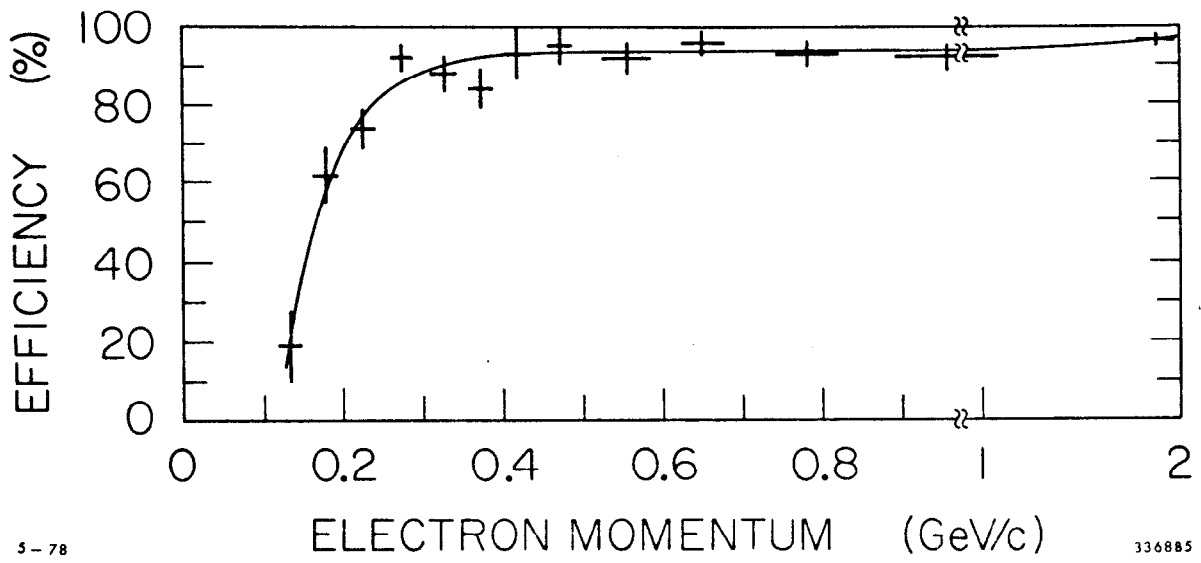


Fig. 2

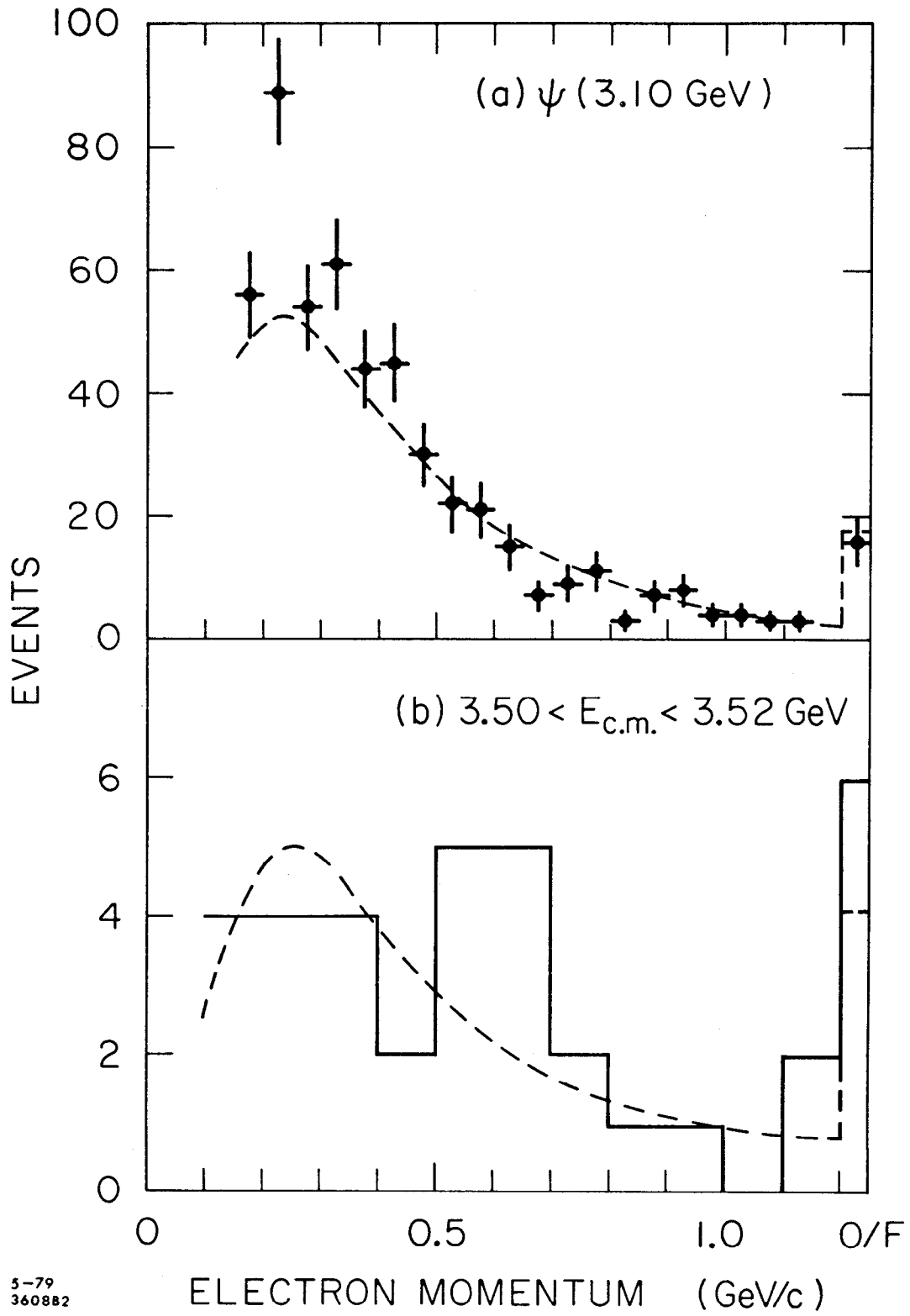


Fig. 3

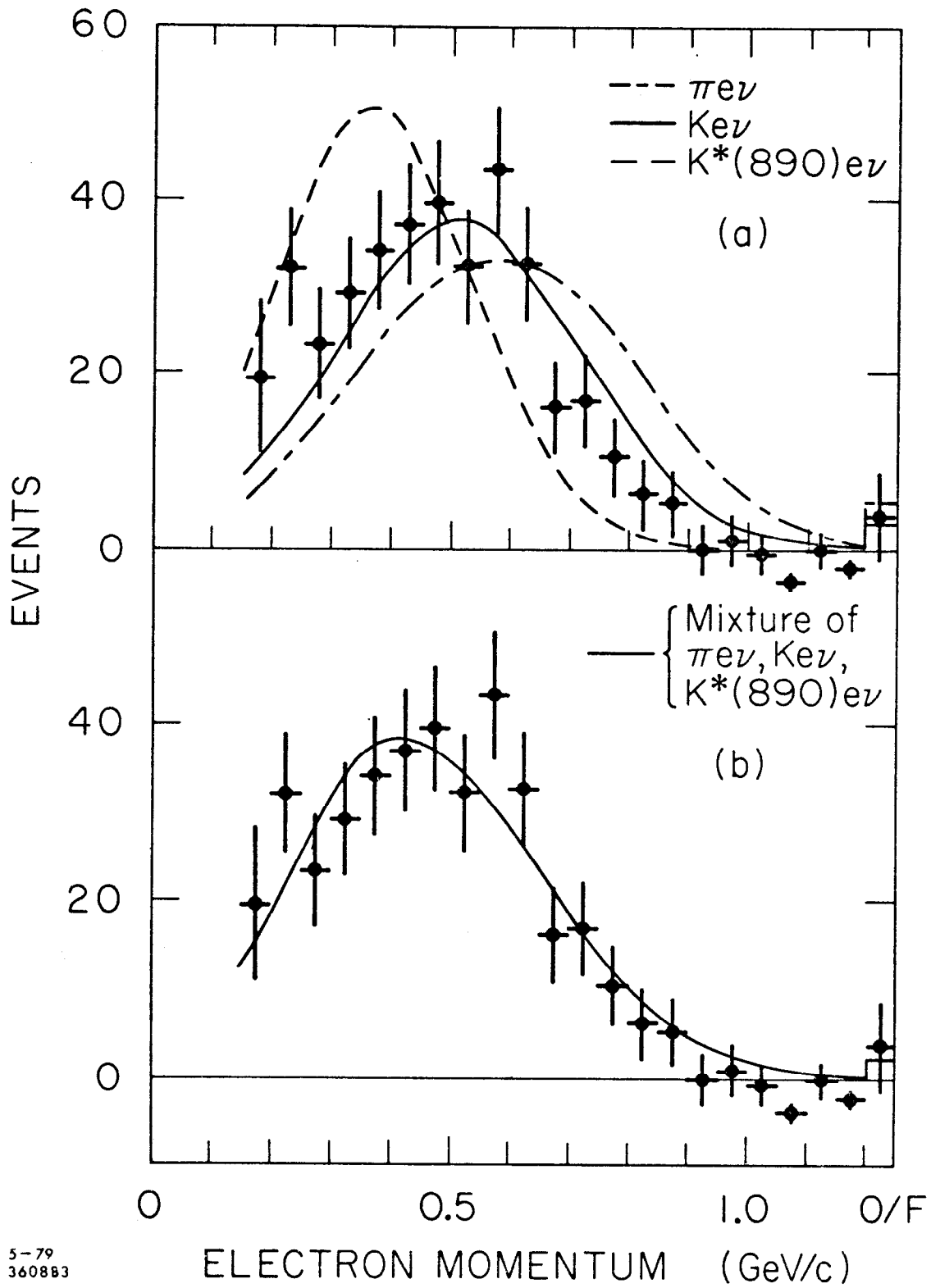


Fig. 4